PAPER

Check for updates

Activated carbon cloth as efficient microporous electrode for maleic acid recovery through electrical potential

Dennis Röcker, [ID] [ab] Fabian Biebl,[a] Lisa Meier, [ID] [ab] Sebastian Patrick Schwaminger, [ID] [cd] Paula Fraga-García [ID] *[a] and Sonja Berensmeier [ID] *[ab]

The purification of biobased organic acids poses considerable challenges due to the high energy demand and associated costs of conventional methods, which hinder the market potential of these renewable carbon sources. This study investigates the charging and electrosorptive behavior of activated carbon cloths for maleic acid as an alternative to the recently proposed particulate and monolithic electrosorptive systems for organic acid recovery. Characterization of the activated carbon cloth (ACC) revealed slightly acidic behavior with a point of zero charge (pHpzc) of 6.18, while Raman spectroscopy confirmed a highly amorphous structure. These features influence both adsorption capacity and charging behavior. Positive potentials increase maleic acid uptake to a maximum of 50.40 mg g^{-1} at +1.00 V *vs.* Ag/AgCl, marking a greater than 5-fold improvement compared to open-circuit conditions. Conversely, negative potentials promote desorption, achieving recoveries of up to 93% at −1.00 V *vs.* Ag/AgCl. While applied potentials enabled precise control over the electrosorptive uptake and recovery of maleic acid, pore diffusion limitations resulted in prolonged kinetics for uptake (∼180 min) and recovery (∼60 min). For background electrolyte concentrations up to 20 mM NaCl, competition from inorganic ions was negligible and did not affect uptake behavior, while higher concentrations facilitated maleic acid release through electrodesorption. Our results demonstrate the potential of ACCs for the electrosorptive recovery of organic acids, even in media with elevated competing ion concentrations. Thus, ACCs offer a promising alternative to conventional purification methods, contributing towards sustainable bioprocessing and industrial applications.

1 Introduction

Organic acids of microbial origin were identified by the Pacific Northwest National Laboratory as a promising source of renewable carbon.[1] While market capitalization is currently small compared to their petroleum-derived counterparts, these biobased chemicals are expected to experience significant market growth as prices become more competitive and global efforts toward green chemistry accelerate.[2] However, recovering and purifying organic acids from microbial sources remains challenging due to the complexity of the fermentation broth.[3,4]

Traditionally, organic acids are recovered *via* crystallization, esterification, or distillation, but these energy-intensive techniques can account for up to 70% of production costs, highlighting the need for more efficient alternatives.[5–9] Blanc *et al.*[10] recently proposed preparative chromatography as an energy-efficient alternative for organic acid recovery. While it offers high yields and purity with reduced energy use, the cost of functionalized resins remains a significant barrier to economic viability.[10,11] Carbon-based adsorbents provide a more cost-effective solution and are widely used in wastewater treatment for pollutant removal.[12] Due to their high surface-to-volume ratio, low cost, and high adsorption capacity, carbon-based sorbents are widespread and studied for a variety of different targeted adsorbates including both inorganic and organic constituents.[13,14] However, a major drawback of activated carbons in adsorption processes is the lack of cost-effective and *in situ* regeneration techniques.[15,16] In this respect, electrochemical methods provide an efficient alternative, as they can be operated with a small footprint, powered by renewable energy

[a] Chair of Bioseparation Engineering, TUM School of Engineering and Design, Technical University of Munich, Boltzmannstraße 15, 85748 Garching, Germany. E-mail: p.fraga@tum.de, s.berensmeier@tum.de

[b] Munich Institute for Integrated Materials, Energy and Process Engineering, Technical University of Munich, Lichtenbergstraße 4a, 85748 Garching, Germany

[c] Division of Medicinal Chemistry, Otto-Loewi Research Center, Medical University of Graz, Neue Stiftingtalstraße 6, 8010 Graz, Austria

[d] BioTechMed-Graz, 8010 Graz, Austria

and allow for *in situ* adsorption and regeneration without additional chemicals.[17] By tuning adsorption properties through the application of electrical potential, these methods enable the simultaneous recovery of adsorbates and regeneration of adsorbents, driven by the formation of an electrochemical double layer (EDL) at the solid–liquid interface.[18] Particulate carbon is often used as electrode material due to its large specific surface area and consequently high capacitance. The pore structure and surface properties of the carbon material are critical in determining both double-layer capacitance and adsorption capacity, which govern the formation of the EDL.[19–21] While macropores facilitate mass transfer, mesopores and micropores predominantly dictate ion adsorption capacity.[22,23] Recent research into electrosorption has shifted towards organic pollutant removal, reflecting the increasing prevalence of organic contaminants in water.[24–26] However, in contrast to the advances in capacitive deionization for inorganic ions, the electrosorption of more structurally complex organic molecules remains challenging due to the multiple weak intermolecular forces that additionally influence adsorption under applied potential.[27]

Brammen *et al.* characterized carbon nanotubes as stationary phase material for electrochemically modulated liquid chromatography (EMLC).[28] A maximum binding capacity of 19.6 µmol maleic acid per g resin was reported at +0.8 V *vs.* Ag/AgCl.[28] However, several factors such as high internal resistance of the particle electrode, parasitic redox reactions and a considerable loss of binding capacity with increasing background electrolyte complicate and limit the efficiency of the proposed process.[14,29] Similarly, Han *et al.* observed reduced electrosorption capacity but increased adsorption rates with rising electrolyte concentrations, highlighting the antagonistic role of inorganic ions.[30] Alternatively, 3D electrodes can be manufactured upon combination with binding agents, realizing a higher packing density and mechanical stability of the electrode material.[31] However, the use of binding agents typically results in a reduction of surface area and binding sites, negatively impacting adsorption performance.[31,32]

To address these limitations, this study investigates the use of activated carbon cloths (ACCs) as free-standing electrodes for the electrosorptive recovery of organic acids. ACCs offer several advantages over particulate or monolithic carbon materials, including a higher specific surface area, excellent ion and electron transport properties, and the ability to function as a self-supporting electrode without the need for binding agents.[33–35] Building on previous research of our group, we systematically analyse the electrosorption behaviour of organic acids on ACCs under varying electrochemical and environmental conditions.[14,28,29,31] This study examines how different electrochemical parameters, and environmental factors govern the adsorption process, influencing both the efficiency and selectivity of organic acid uptake. Additionally, we analyze the kinetics of electroadsorption and desorption, providing insights into the mechanisms that control adsorption rates and regeneration efficiency. Special emphasis is placed on the role of inorganic ions, assessing their effect on the uptake

behavior and charging characteristics of ACC electrodes. By addressing these aspects, this research enhances the fundamental understanding of organic acid electrosorption and contributes to the application of ACC-based electrodes in industry. Ultimately, this work supports the development of a cost-effective and scalable approach for organic acid recovery, offering an efficient alternative to conventional adsorbents as well as process diversification alternatives for future bioseparation technologies.

2 Experimental

2.1 Material preparation and characterization

Activated carbon cloths (ACC) were acquired from Kynol Europe GmbH (ACC-5092-10, Hamburg, Germany). Prior to use, the ACC were washed in Acetone (ACS reagent, Merck KGaA, Darmstadt, Germany) for 30 min at room temperature to remove impurities. Afterwards the acetone was discarded, and the ACC were washed twice in DI-H_2O for 10 min at room temperature and finally dried overnight at 60 °C. Subsequently, the ACC were stored in a dried state until utilization. The pH drift method was utilized to investigate the charging characteristics of the carbon material. For this purpose, solutions of 10 mM NaCl (Merck KGaA, Darmstadt, Germany) were adjusted to an initial pH ranging from 4 to 9 by addition of 1 M HCl (Merck KGaA, Darmstadt, Germany) or 1 M NaOH (Merck KGaA, Darmstadt, Germany). The prepared solutions were purged with N2 and a rectangular piece (3×3 cm^2) of ACC added to 50 mL of purged solution. Then, the samples were incubated at room temperature for 24 h under N_2 atmosphere. Afterwards, the pH drift was measured for three individual samples for each initial pH. For scanning electron microscopy (SEM) a Philips XL 40 (Philipps, Amsterdam, Netherlands) was used at a voltage of 20 kV. Nitrogen adsorption isotherms were conducted using a Quantachrome Surface Analyzer (Quantachrome Autosorb IQ, Quantachrome Inc., Boynton Beach, USA) at 77 K in volumetric adsorption mode. Prior to dosing with nitrogen, the real density of the sample was determined with helium pycnometry. The BET surface was determined within the $p/p0$ range of 0.05 to 0.35. Raman spectroscopy was conducted on a Renishaw invia Reflex Raman System (Renishaw, Wotton-under-Edge, UK) at a wavelength of 532 nm and 10% laser intensity.

2.2 Electrochemical characterization

All experiments of applied potential were conducted using a Gamry Interface 1000E (Gamry, Warminster, USA) operated in surface mode. Potentials were applied against an Ag/AgCl reference electrode (LF-1-45, Innovative Instruments Inc., Tampa, USA) with NaCl background concentration ranging from 0 mM to 20 mM. A series of double pulsed chronoamperometries was conducted with a step size of ± 0.10 V *vs.* Ag/AgCl ranging from 0.10 V to 1.00 V for 15 min in each step. Chronocoulometric experiments were performed at a potential of 0.50 V *vs.* Ag/AgCl for 30 min. Afterwards discharging was

monitored at open circuit potential (OCP). The time constant τ for capacitive charging was defined according to eqn (1) and (2):

$$Q(t) = C \cdot V \left(1 - \exp\left(\frac{-t}{\tau}\right)\right) \qquad (1)$$

$$\tau = -\frac{\mathrm{d}t}{\mathrm{d}\ln\left(1 - \frac{Q}{Q_0}\right)} \qquad (2)$$

where Q represents the accumulated charge over time, C the capacitance of the cloth and V the applied voltage. Cyclic voltammetries (CVs) were conducted at scan rates of 1 mV s^{-1}, 10 mV s^{-1}, 50 mV s^{-1} and 100 mV s^{-1} in a potential range between -1.00 and $+1.00$ V vs. Ag/AgCl.

2.3 Sorption experiments

Adsorption experiments of maleic acid (Merck KGaA, Darmstadt, Germany) without applied potential were conducted for initial concentrations ranging from 1 mM to 100 mM. The pH of the solutions was adjusted to pH 5, 7, or 9 by addition of 1 M NaOH or 1 M HCl. Afterwards, 5 mm (4.5 mg) cutouts of the ACC were incubated in 200 μL maleic acid solution overnight (room temperature, 800 rpm) and the uptake of maleic acid was determined for three individual samples by UV/Vis spectroscopy at a wavelength of 262 nm (Nanodrop, Implen GmbH, Munich, Germany). Kinetics for maleic acid uptake were investigated for an initial concentration of 10 mM maleic acid adjusted to a pH of 7. The uptake of maleic acid was determined at an elapsed time of 0, 1, 5, 10, 30, and 60 minutes. For the desorption experiments, the ACC were incubated in 10 mM maleic acid at pH 7 until equilibrium was reached (4 h). Afterwards, unbound maleic acid was removed by washing the ACC twice with 200 μL of DI-H$_2$O. Desorption kinetics were then investigated by transferring the ACC into 200 μL of 1 M NaCl for up to 60 minutes at room temperature and 800 rpm. Potential controlled interactions were investigated in a 3D printed (Clear V4, Formlabs GmbH, Berlin, Germany) H-cell using a cation exchange membrane (CMI-7000S, Membranes International Inc., Ringwood, USA) as separator. Rectangular (3 $\times$ 3 cm^2) pieces of ACC were contacted as working electrode. Adsorption experiments were conducted against an Ag/AgCl reference electrode. Applied potentials were varied between OCP and $+1$ V vs. Ag/AgCl using a Gamry Interface 1000e potentiostat (Gamry, Warminster, USA). For desorption experiments 10 mM maleic acid was first electrosorbed at an applied potential of $+0.5$ V vs. Ag/AgCl until equilibrium was reached (3 h). Afterwards the ACC was removed and washed twice with 8 mL of DI-H$_2$O. Afterwards, negative potentials ranging between OCP and -0.75 V vs. Ag/AgCl were applied for maximally 60 min. For all electrosorption experiments the concentration of maleic acid was determined by UV/Vis spectroscopy at a wavelength of 262 nm for the adsorption and 230 nm for the desorption. The experiments were conducted with NaCl background concentrations of 0 mM, 10 mM and 20 mM. The adsorption kinetics were fitted using a pseudo first order

expression according to eqn (3):

$$\frac{\mathrm{d}q}{\mathrm{d}t} = k_1 \cdot (q_{\mathrm{eq}} - q) \qquad (3)$$

where k_1 represents the pseudo first order rate constant. The adsorbed amount of adsorbate onto the adsorbent at equilibrium is q_{eq} and q represents the adsorbed amount of adsorbate adsorbed at a given time t.

3 Results and discussion

The activated carbon cloth used in this study consists of a network of highly ordered and developed fibers arranged as a woven fabric. The individual fibers exert a diameter of roughly 15 μm (Fig. 1(a)). The highly microporous nature of the ACC is confirmed through N$_2$ adsorption measurements, see data in Fig. 1(b). A total pore volume of 0.48 cm^3 g^{-1} correlating to an average pore size of 2.65 nm was measured for the ACC. The specific surface area was determined to 734 m^2 g^{-1}. To study the charging behaviour of the ACC in aqueous solution without any applied potential, the pH drift method was utilized.[14] When placed in aqueous solution, functional groups on the ACC surface undergo protonation or deprotonation depending on the solution pH, impacting the adsorption of OH$^-$ and H$^+$ ions. At a pH of 6.18 no difference between the initial pH and the pH after incubation of the ACC was observed, indicating the pHpzc of the material (Fig. 1(c)). Above the pHpzc, a shift towards more acidic values is observed as functional groups on the carbon surface deprotonate. Below the pHpzc, active groups protonate, and the pH of the solution is shifted to a more alkaline value. With a pHpzc of 6.18, the studied ACC behaves slightly acidic, which corresponds well to other carbon materials utilized in this field.[36] Raman spectroscopy provides additional insight into the ACC structure (Fig. 1(d)). In raw graphite, the characteristic band at 1605 cm^{-1} corresponds to vibrations of sp^2-hybridized carbon atoms. The band visible at 1335 cm^{-1} is associated with sp^3-hybridized carbon atoms and in the case of raw graphite indicates structural defects within the delocalized π-system. The intensity ratio ($I_{\mathrm{D}}/I_{\mathrm{G}}$ = 0.91) reveals a highly amorphous structure of the individual fibers within the utilized carbon cloth. This aligns well with the previously observed pH drift, suggesting a variety of oxidized carbon atoms on the surface.[37,38] While these functional groups provide possible sites of adsorption and interaction with analytes, the reduction of in-plane sp^2 domains further affects the conductivity of the fibers and thus influences the electrical charging behaviour of the utilized ACC.[39]

Carbon cloths are widely studied for their application in electric double layer capacitors (EDLC), where high concentrated electrolyte solutions are typically employed to achieve efficient ion adsorption and charge storage.[40] However, their performance in low-concentration electrolytes, as found in fermentation broths with residual NaCl is commonly not of interest.[41,42] Lower ionic strengths significantly influence charging kinetics, potentially prolonging charging and adsorption times.[43] Thus, we investigate the charging behaviour of the ACC
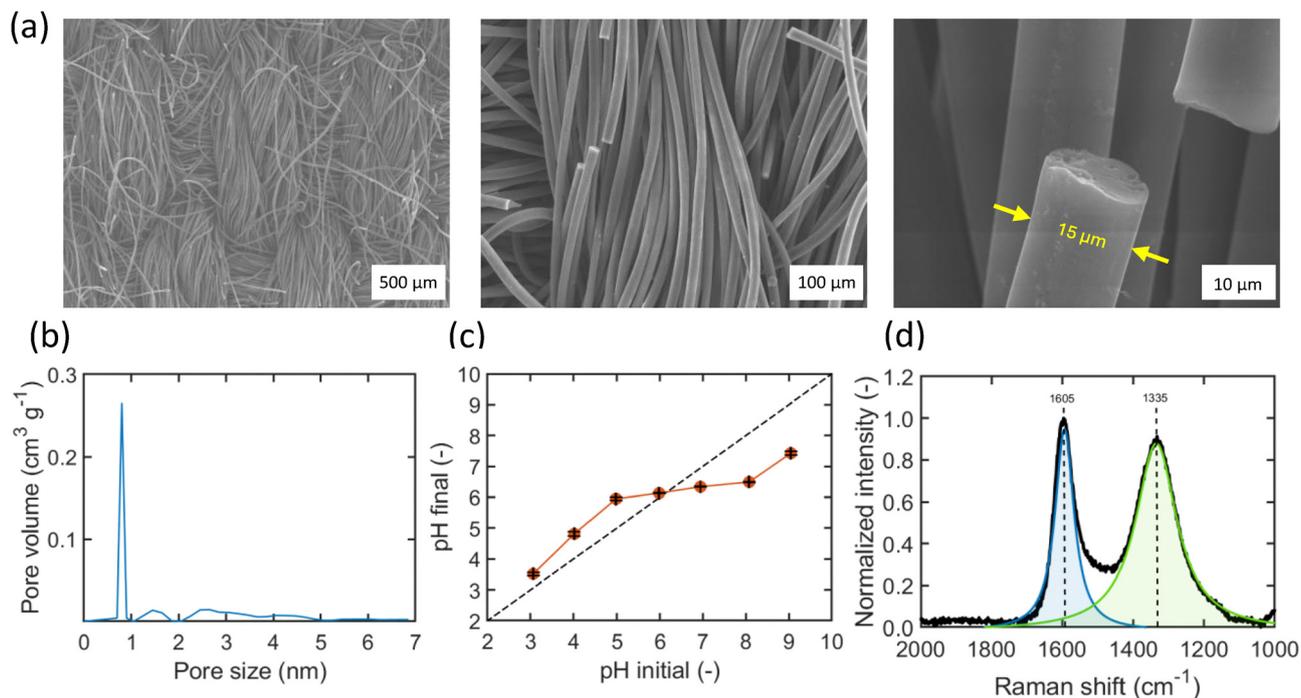
Fig. 1 Material properties of the utilized activated carbon cloth. SEM images (a) taken at 20 kV for a magnification of 100×, 500× and 5000×. Pore size distribution calculated through N2 adsorption isotherms (b). Influence of the cloth on the aqueous environment investigated through pH drift experiments (c) as well as Raman spectra (d) of the D- (1355 cm^{-1}) and G-band (1595 cm^{-1}) of the ACC taken at 10% laser intensity at a wavelength of 532 nm.
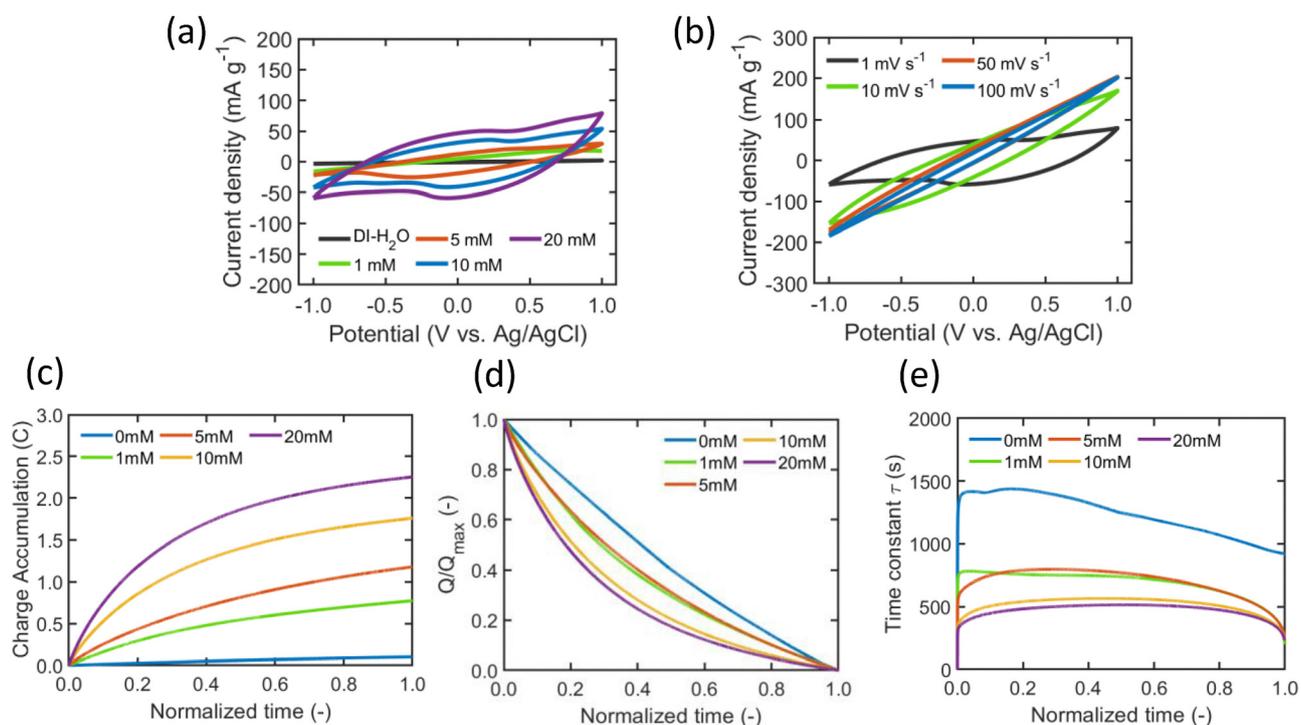

Fig. 2 Charging behaviour of ACCs under various environmental conditions: (a) influence of background electrolyte concentration at a constant scan rate of 1 mV s^{-1}, (b) influence of scan rate at a constant electrolyte concentration of 20 mM NaCl (c) accumulated charge (d) normalized charge progression (e) time constant changes during the charging process. All experiments were conducted against an Ag/AgCl reference electrode.

for varying concentrations of NaCl ranging from DI-H$_2$O to 20 mM NaCl as background electrolyte (Fig. 2(a)–(e)).

In dilute concentrations of NaCl the cyclic voltammograms (CVs) show capacitive behaviour characterized by high resistance and diffusion limitations (Fig. 2(a)). This is evidenced by distortions in the typically rectangular shape of ideal EDLCs. At concentrations below 5 mM NaCl, the ACC shows negligible charge storage or capacitive response, attributed to high internal resistance and electrolyte starvation. Here, conducting ions become adsorbed within the double layer, reducing electrolyte conductivity.[44] With increasing NaCl concentrations, the area capacitance of the ACC electrodes considerably increases, showing the strong impact of ionic transport on the charging behaviour. In contrast, increasing the scan rate from 1 mV s^{-1} to higher values results in a strong reduction of ion diffusion, as the effective area of the ACC for EDL formation is reduced.[45] Similar trends can be observed with chronocoulometries as the accumulated charge on the electrodes surface as well as the time constant for the charging process strongly depends on the residual background electrolytes concentration (Fig. 2(c)–(e)). At dilute electrolyte concentrations, high time constants (τ) reflect limited charge transfer. As the concentration increases, this limitation is mitigated, and the time constant decreases.[46] Furthermore, a distinct progression of τ can be observed as time progresses. Initially, large pores and easily accessible surface sites are occupied resulting in an initially reduced time constant. With progressing time the system transitions to a diffusion-controlled regime where diffusion path lengths to smaller pores increase, resulting in higher charge transfer resistance and reduced mobility of the ions within the confined space of the ACC's micropores.[46] Towards the end, the charging process is no longer dominated through diffusion through the porous network, as indicated by a sharp decrease in τ.[47] These findings provide valuable insight into the mechanisms underlying ion adsorption and transport within the porous structure of the material. In comparison to particulate or binder-comprising monolithic carbon electrodes the interwoven fibers benefit from facilitated charge transport.[14,29,31] Nevertheless, the highly microporous nature of the ACC indicates a charging

process that is largely diffusion-limited, suggesting a significant impact also on electrosorption kinetics. Building upon this understanding, we investigated the adsorption behaviour of the target organic acid, maleic acid, onto the ACC. By conducting adsorption isotherms under varying pH conditions, we sought to elucidate the influence of surface charge and molecular interactions on the material's performance in capturing organic acids. The adsorption behaviour without applied potential was investigated with analyte concentrations ranging from 0 to 100 mM (Fig. 3(a)). A strong dependence of the pH on the adsorption behaviour is visible showing that both the protonation state of the ACC (Fig. 1(c)) as well as the dissociation state of the targeted organic acid (Fig. 3(c)) play a critical role in the adsorption onto the carbon material. At a pH of 9 in which maleic acid carries a charge of $-2e$ and the cloth is negatively charged as well, a maximal uptake of 10.72 mg g^{-1} maleic acid is observed. Decreasing the pH leads to the subsequent increase in maleic acid uptake. At pH 7 we observe a maximal load of 31.07 mg g^{-1}. At pH 5, with the ACC carrying a positive net charge and maleic acid carrying a charge of $-1e$, the uptake considerably increases up to 128.71 mg g^{-1} with no saturation behaviour observable. We assume enhanced electrostatic interactions to be the major driving force of maleic acid adsorption. However, several other interactions complement the process such as hydrogen bonding between oxygen functionalities and the carboxylic groups of maleic acid as well as π-interactions between the graphitic ACC backbone and the conjugated C-bond of maleic acid, allowing for adsorption under electrostatically unfavourable conditions.[48,49] Similar observations were made by Trunzer et al. and Wagner et al. who observed a roughly 10 times higher adsorption capacity for particulate activated carbon compared to other carbon structures such as carbon nanotubes.[29,50] Both surface charge and surface area show considerable influence on the adsorption behaviour. Trunzer et al. reported a pHpzc of ~3.5 for CNTs indicating a non-electrostatically driven adsorption behaviour over a broad pH range, dictated by the presence of a multitude of defects within the graphitic structure of the utilized CNT.[14] The ACC shows a fast uptake of maleic acid with the adsorption
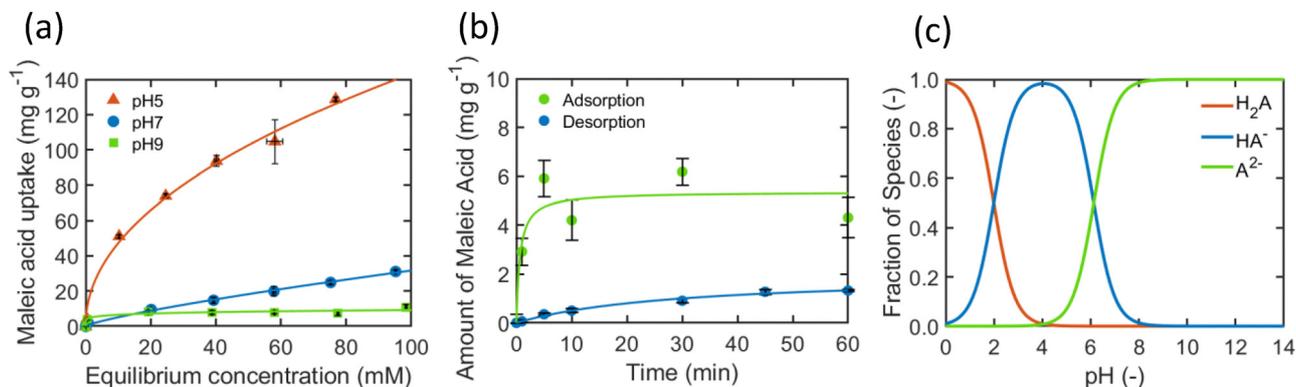
Fig. 3 Adsorption isotherms (a) of maleic acid at a pH of 5, 7 and 9, as well kinetics (b) for the adsorption of 10 mM maleic acid at pH 7 and subsequent desorption in the presence of 1 M NaCl. Dissociation behavior of maleic acid (c) in dependence of the environmental pH. Experiments were conducted on three individual samples respectively.

being completed within 10 minutes for the incubation of ACC at pH of 7 and a maleic acid concentration of 10 mM (Fig. 3(b)). At low equilibrium concentrations as investigated here, no competition at the surface is expected due to the ACC's large specific surface area. Thus, the adsorption process is only determined by the electrostatic state of both the adsorbent's surface and the analyte. In this case, the adsorption kinetics follow a Lagergren behavior.[51–53] In addition to fast adsorption kinetics, an effective desorption is a critical characteristic for the suitability of the ACC material for a recovery process. In comparison to the potential dependent elution, we studied the elution behaviour of maleic acid with 1 M NaCl as effective way to screen double layer interactions and mitigate electrostatic attraction. A total recovery of 34% of the bound maleic acid could be gained with immersion of the loaded cloth in 1 M NaCl. Desorption kinetics in contrast to the adsorption are relatively slow. Hoppen *et al.* observed a similar trend, studying the desorption of acetylsalicylic acid from particulate activated carbon over a period of 6 hours without reaching equilibrium.[54] These effects are likely due to mass transport limitations within the highly microporous structure when the double layer is screened with 1 M NaCl. As both adsorption capacity and desorption kinetics offer room for improvement, it is important to analyse the influence of an additional factor on the sorption process. Hence, we investigated the potential dependent adsorption and desorption kinetics in the next step (Fig. 4). The reaction time constants are summarized in Table 1.

The adsorption at open circuit potential (OCP) shows fast saturation with a maximal loading of 9.62 mg g^{-1} reached within the first 30 minutes. No further uptake occurs after this point. When a negative potential of -0.25 V *vs.* Ag/AgCl is applied, electrostatic repulsion between the ACC and maleic acid leads to a reduction in uptake by 45%, with the maximum uptake decreasing to 4.86 mg g^{-1}. However, further increase of the negative applied potential does not result in further reduction of maleic acid uptake. Specifically, at -0.5 V *vs.* Ag/AgCl and -0.75 V *vs.* Ag/AgCl, the uptake remains constant at 4.67 mg g^{-1} and 5.09 mg g^{-1}. This behaviour suggests that additional interaction mechanisms, cannot be overcome only by application of low electrical potentials.[50,55] These occurrences are important to consider when further investigating the regeneration and separation behaviour. In contrast, applying positive potentials strongly increases the overall binding capacity of the ACC. With $+0.25$ V *vs.* Ag/AgCl the uptake is effectively doubled to 20.21 mg g^{-1}. As the applied potential further increases, the uptake reaches a maximum of 51.27 mg g^{-1} at $+1.00$ V *vs.* Ag/AgCl. However, previous studies have shown that prolonged application of positive potentials can lead to electrochemical oxidation of the carbon surface, potentially altering surface chemistry and affecting electrosorption performance.[29,56] The strong dependence of maleic acid partitioning on the ACC surface as a function of applied potential becomes evident (Fig. 4(b)). While at OCP around 80% of the organic acid are still dissolved in solution, the amount of unbound maleic acid strongly decreases with applied potential until most of the analyte is bound on the surface of the ACC. This results in a
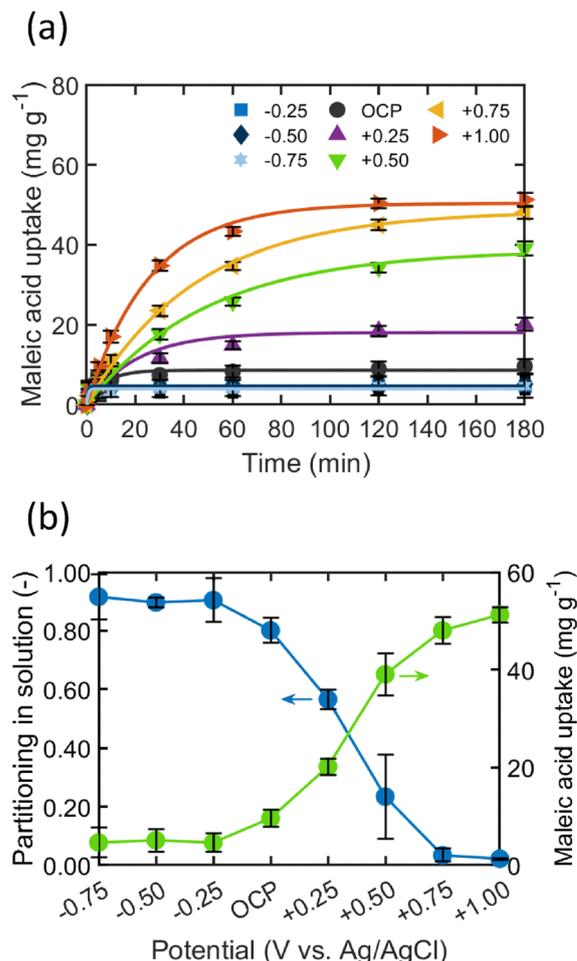

(a)

(b)

Fig. 4 Electrosorption kinetics of 10 mM maleic acid at pH 7 onto ACC for various applied potentials (a) and maleic acid partitioning (b) onto the ACC. Experiments were conducted against an Ag/AgCl reference electrode for three individual samples respectively.

Table 1 Kinetic parameters for electrosorption of maleic acid onto ACC at different applied potentials

Potential (V *vs.* Ag/AgCl)	Pseudo first order kinetics			
	q_{eq} (mg g^{-1})	q_{eq} (molecules nm^{-2})	K_1 (min^{-1})	R^2
-0.75	4.668	0.0327	1.598	0.85
-0.50	5.091	0.0360	1.555	0.94
-0.25	4.856	0.0326	2.428	0.99
OCP	9.617	0.0680	0.135	0.93
$+0.25$	20.21	0.1428	0.049	0.89
$+0.50$	39.06	0.2761	0.020	0.98
$+0.75$	48.06	0.3397	0.022	0.99
$+1.00$	51.27	0.3624	0.039	0.99

maximal uptake of 0.36 molecules of maleic acid per nm^2 cloth at $+1$ V *vs.* Ag/AgCl and correlates to roughly 27% of monolayer coverage. These phenomena are also reflected in the adsorption kinetics. Faster diffusion rates and lower loadings are observed for negative potentials as micropores become increasingly negatively charged and do not partake in the adsorption process.

Conversely, positive potentials lead towards reduced time constants as electrostatic forces allow for covering of the surface condensed within the mostly microporous structure of the ACC. Given the slow charging dynamics observed through chronocoulometry (Fig. 2), the process appears limited by pore diffusion. Interestingly, Han *et al.* and Bayram *et al.* reported increasing time constants with the transition from repulsive to attractive electrical potentials.[30,57] A maximal adsorption rate of 0.082 min^{-1} at +0.7 V *vs.* SCE was reported by Han *et al.* for the adsorption of phenol onto activated carbon fibers.[30] However, adsorption rates on carbon surfaces can drastically vary depending on pore structure, target analyte and environmental conditions.[58–60] Various models, including pseudo-first and pseudo-second order, are used for the prediction of time constants and general comparison between different processes is rarely conclusive. In our case we observe a fast initial step of adsorption towards the carbon surface, followed by a relatively slow step which we explain by diffusion into smaller pores and relate to Lagergren behaviour.[61,62] The use of electrical potential is mostly studied for adsorption processes.[30,57,63] However, limited data exists on the kinetics governing the desorption process from polarized electrodes for organic constituents, which we present in Fig. 5 and Table 2.[36,64]

Switching to OCP after electrosorption only leads to a release of maximally 2.69 mg g^{-1}, which correlates to 6% recovery. However, potential inversion to negative applied potentials leads to effective recovery of large fractions of the previously adsorbed maleic acid. Approximately 68% of maleic acid were released within 60 minutes of an applied potential of −0.25 V *vs.* Ag/AgCl. Further increase of the applied potential led to a recovery of 93% within 60 minutes of applied potential. Nonetheless, considering the uptake at negative applied potential in previous electrosorption experiments, a complete elution with increased time or elevated potential seems highly unlikely as non-electrostatic interactions are still likely to occur.[36] In comparison to regeneration through chemical or thermal treatment, electrical potential allows for *in situ* regeneration and is thus likely more energy and resource efficient.[15,16] The observed recoveries for maleic acid align with previous studies on electrodesorption of thiocyanate and arsenate under applied potential, where recoveries of over 90% have also been reported, demonstrating the advantages of *in situ* regeneration of carbon electrodes.[36,65] The applied potential strongly influences desorption rates, as shown in Table 2. Moving from −0.25 V *vs.* Ag/AgCl to −1.00 V *vs.* Ag/AgCl the rate constant increases from 0.019 min^{-1} to 0.052 min^{-1} indicating higher electrostatic repulsion between the carbon electrode and the previously adsorbed organic acid. Interestingly, the rate constant is found highest under OCP conditions. However, as the cloth is highly microporous we expect a large degree of adsorbed maleic acid still bound within its porous structure, while the released molecules might originate from the more solute accessible surface.[46] Thus, recovery times of over 60 minutes are commonly observed regardless of the nature of the analyte, considerably decreasing the productivity of the electrosorptive processes.[36,65]
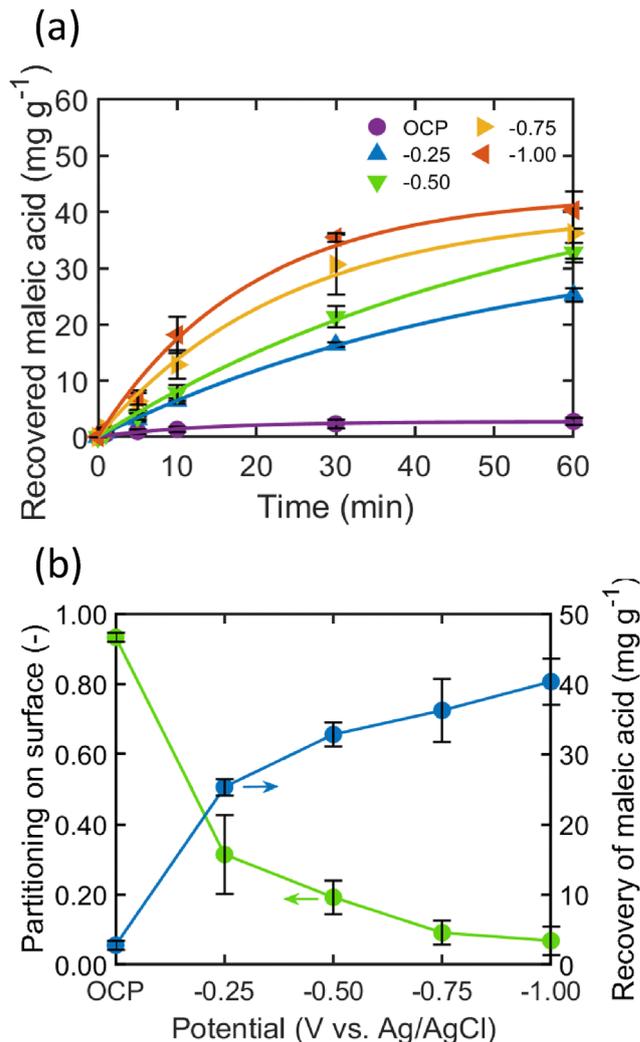

Fig. 5 Electrodesorption kinetics of maleic acid from ACC at OCP compared to various applied potentials (a) and partitioning of maleic acid (b). 10 mM maleic acid at pH 7 were electrosorbed at +0.5 V *vs.* Ag/AgCl for 3 h. A final capacity of ∼40 mg g^{-1} was reached after the electrosorption step. Prior to electrodesorption the ACC were washed twice in 8 mL of DI-H$_2$O. All experiments were conducted against an Ag/AgCl reference electrode for three individual samples respectively.

In contrast to organic acids, the electrosorption of inorganic ions has been highly studied.[66] These ions are considerably smaller and profit from higher diffusivities, charge density and loading on the carbon electrodes.[14] However, since inorganic

Table 2 Kinetic parameters for the recovery of maleic acid from ACC at different applied potentials

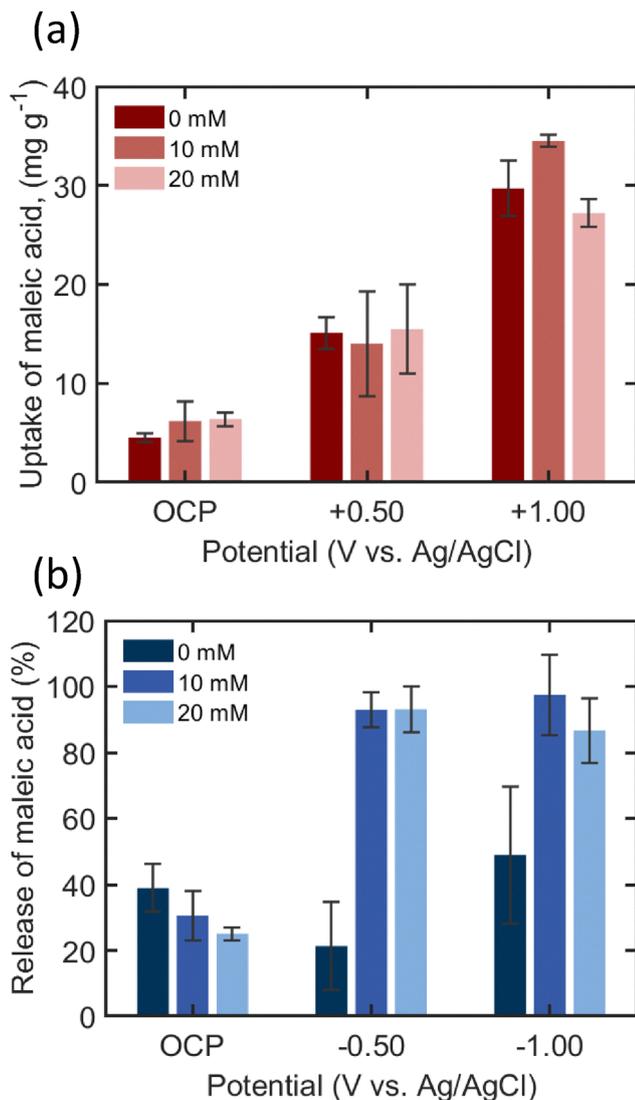| Potential (V *vs.* Ag/AgCl)	Electrosorbed (mg g^{-1})	Pseudo first order kinetics		
		q_{eq} (mg g^{-1})	K_1 (min^{-1})	R^2
OCP	40.82	2.75	0.0748	0.97
−0.25	37.54	25.29	0.0193	0.99
−0.50	40.76	32.78	0.0179	0.99
−0.75	39.73	36.21	0.0419	0.99
−1.00	43.20	40.32	0.0519	0.99

(a)

(b)

Fig. 6 Uptake (a) of 10 mM maleic acid at pH 7 under varying NaCl concentrations and release (b) for different applied potentials combined with varying NaCl background concentrations. Uptake and release were measured after 30 min of adsorption and desorption respectively. All experiments were conducted against an Ag/AgCl reference electrode for three individual samples.

ions are integral components of most natural systems, they directly compete with organic acids for adsorption sites.[67,68] We investigated the influence of NaCl concentration as background electrolyte on the uptake and release of maleic acid on the activated carbon cloth (Fig. 6). Under OCP conditions no significant change in maleic acid can be observed with increasing the NaCl background concentration from 0 mM to 20 mM. However, when an electrical potential was applied, the uptake of maleic acid increased consistently, regardless of the NaCl concentration. In contrast Han *et al.* observed a considerable decrease in analyte uptake when investigating the electrosorption of phenol in the presence of Na_2SO_4.[30] While the uncompensated resistance of the soaked electrode and solution decreases and a more efficient charging of the carbon electrode

is enabled (Fig. 2), competition on the surface, depending on the process time, favours either the ion with higher diffusivity or charge density.[69] In our case, the ratio between analyte and background electrolyte is kept high with values of 1:1 or 1:2, respectively. In comparison to studies targeted on *e.g.* pollutant removal, observing a significant decrease, this ratio is up to 50 times higher.[29,30,36]

This clearly demonstrates the importance of finding a balance between enhancing adsorption kinetics and the competition of the ions on the surface. For the recovery of dilute species this ratio is crucial in determining overall process efficiency.[29,70,71] However, fermentation titres of organic acid usually comprise concentrations of 50 g L^{-1} and higher while background electrolyte concentrations typically are in a low molarity ranging from 10 mM to 100 mM.[42,67,72] Hence, we expect reasonable upconcentration for the capacitive recovery of organic acids, when operated in recirculated batch mode in comparison to previously suggested pulse injections.[14,29] Moreover, desorption is strongly influenced by the concentration of background electrolyte in the media (Fig. 6(b)). In the absence of background electrolyte, the recovery of maleic acid varied only slightly with applied potential, indicating that the high resistance within the porous carbon electrode and surrounding media hindered effective surface charging. With increasing the background concentration from 0 mM to 10 mM, the recovery of maleic acid at −0.50 V *vs.* Ag/AgCl improved substantially, from 21% to 93%. Both the efficient electrical charging as well as the displacement of surface-bound maleic acid by Cl^- anions act in favour of the maleic acid desorption from the carbon electrode. Further increases in the applied negative potential did not result in higher recoveries, suggesting that other factors, such as non-electrostatic interactions, might limit complete desorption. Our results suggest that efficient recovery of maleic acid is possible even in the presence of moderate background electrolyte concentrations. However, further optimization of process conditions, including the balance of electrolyte concentration and applied potential, is essential to improve the efficiency and scalability of this method. A future concept should envision utilizing the microporous ACC as flow through electrode while cycling the fermentation feed stock, thereby levering out the slow electrosorption kinetics investigated in this paper. An elegant concept for incorporating ACCs as streamed-through working electrode has been already proposed by Bayram *et al.* and could be further improved by increasing packing density, placement of the counter electrode outside of the permeate stream, and a more homogeneous contacting of the ACC.[71]

4 Conclusions and outlook

Activated carbon cloths as freestanding electrodes for electrosorptive organic acid recovery offer several advantages over particulate electrode systems. This study provides a comprehensive characterization of the charging and electrosorption dynamics of maleic acid on activated carbon cloths under

various environmental conditions and applied electrical potentials. Our findings highlight the critical role of the electrostatic environment for electrosorption as well as the physicochemical interactions between the organic acid and the charged carbon surface. Adsorption was found to be strongly dependent on the solution pH reflecting the impact of protonation of both the analyte and the ACC. Positive applied potentials enhanced adsorption up to 5-fold due to strong electrostatic attraction, while negative potentials did not fully suppress the uptake, indicating that non-electrostatic interactions also play a role. Upon potential inversion high recoveries up to 93% could be achieved with an applied potential of -1.00 V $vs.$ Ag/AgCl. The electroadsorption and electrodesorption kinetics followed pseudo-first-order behaviour with increasing rate constant in dependence of the applied potential. Electrosorption kinetics indicate diffusion limitations within the microporous structure, with processing times ≥ 60 minutes. Desorption efficiency increased with increasing ionic strength due to improved conductivity and ionic displacement, emphasizing the need to balance solution conductivity and competition in adsorption. Our findings underscore the potential of ACC for the electrosorptive recovery of small organic acids. However, further investigation is necessary, to enhance both efficiency and kinetics. To achieve industrial applicability, the cloths need to be efficiently incorporated in a preparative electrochemical cell allowing for a high packing density and consequently high loading capacities while minimizing parasitic side reactions and the formation of by-products. Furthermore, the electrosorption behaviour with complex fermentation broths is essential to evaluate the selectivity for organic acids in the presence of competing ions and other organic constituents. Since bio-based organic acids are important to sustainable chemical manufacturing, the improvement of electrosorptive techniques remains valuable for the progress of green and effective biorefinery processes.

Declaration of generative AI and AI-assisted technologies in the writing process

During the preparation of this work the authors used GPT-4o to improve the language and clarity within the manuscript. After using this tool, the authors reviewed and edited the content as needed and take full responsibility for the content of the published article.

Author contributions

Dennis Röcker: conceptualization, methodology, validation, formal analysis, investigation, data curation, visualization, writing – original draft, writing – review & editing. Fabian Biebl: conceptualization, methodology, validation, formal analysis, investigation, data curation. Lisa Meier: conceptualization, methodology, validation, formal analysis, investigation data curation. Paula Fraga-García: conceptualization, methodology,

supervision, writing – review & editing. Sebastian P. Schwaminger: conceptualization, writing – review & editing, supervision. Sonja Berensmeier: conceptualization, resources, writing – review & editing, supervision, project administration, funding acquisition.

Conflicts of interest

The authors declare that they have no known competing financial interests or personal relationships that could have appeared to influence the work reported in this paper.

Data availability

The data for this article is available at **https://doi.org/10.17632/rsknbh47zw.1**.

Acknowledgements

References

1 T. Werpy and G. Petersen, *Top value added chemicals from biomass: volume I – results of screening for potential candidates from sugars and synthesis gas*, 2004.

2 Z. Ali, J. Ma and R. Sun, Scaling up clean production of biomass-derived organic acids as a step towards the realization of dual carbon goals: a review, *Green Chem.*, 2024, **26**, 11061–11082.

3 N. A. S. Din, S. J. Lim, M. Y. Maskat, S. A. Mutalib and N. A. M. Zaini, Lactic acid separation and recovery from fermentation broth by ion-exchange resin: A review, *Bioresour. Bioprocess.*, 2021, **8**, 31.

4 K.-K. Cheng, X.-B. Zhao, J. Zeng, R.-C. Wu, Y.-Z. Xu, D.-H. Liu and J.-A. Zhang, Downstream processing of biotechnological produced succinic acid, *Appl. Microbiol. Biotechnol.*, 2012, **95**, 841–850.

5 B. Rukowicz, Electrodeionization for the Bio-Succinic Acid Production Process, *ACS Sustainable Chem. Eng.*, 2023, **11**, 11459–11469.

6 Y. Xiao, Z. Zhang, Y. Wang, B. Gao, J. Chang and D. Zhu, Two-Stage Crystallization Combining Direct Succinimide Synthesis for the Recovery of Succinic Acid From Fermentation Broth, *Front. Bioeng. Biotechnol.*, 2019, **7**, 471.

7 H. G. Joglekar, I. Rahman, S. Babu, B. D. Kulkarni and A. Joshi, Comparative assessment of downstream processing options for lactic acid, *Sep. Purif. Technol.*, 2006, **52**, 1–17.

8   X. Sun, Q. Wang, W. Zhao, H. Ma and K. Sakata, Extraction and purification of lactic acid from fermentation broth by esterification and hydrolysis method, *Sep. Purif. Technol.*, 2006, **49**, 43–48.

9   L. Handojo, A. K. Wardani, D. Regina, C. Bella, M. T. A. P. Kresnowati and I. G. Wenten, Electro-membrane processes for organic acid recovery, *RSC Adv.*, 2019, **9**, 7854–7869.

10 C.-L. Blanc, M.-A. Theoleyre, F. Lutin, D. Pareau and M. Stambouli, Purification of organic acids by chromatography: Adsorption isotherms and impact of elution flow rate, *Sep. Purif. Technol.*, 2015, **141**, 105–112.

11 P. I. Omwene, Z. B. Öcal, M. Yağcıoğlu, A. Karagündüz and B. Keskinler, Novel chromatographic purification of succinic acid from whey fermentation broth by anionic exchange resins, *Bioprocess Biosyst. Eng.*, 2022, **45**, 2007–2017.

12 M. Nasrollahzadeh, M. Sajjadi, S. Iravani and R. S. Varma, Carbon-based sustainable nanomaterials for water treatment: State-of-art and future perspectives, *Chemosphere*, 2021, **263**, 128005.

13 M. Mariana, H. P. S. Abdul Khalil, E. B. Yahya, T. Alfatah, M. Danish and M. Amayreh, Recent advances in activated carbon modification techniques for enhanced heavy metal adsorption, *J. Water Process Eng.*, 2021, **43**, 102221.

14 T. Trunzer, P. Fraga-García, M.-P. A. Tschuschner, D. Voltmer and S. Berensmeier, The electrosorptive response of a carbon nanotube flow-through electrode in aqueous systems, *Chem. Eng. J.*, 2022, **428**, 131009.

15 E. Gagliano, M. Sgroi, P. P. Falciglia, F. G. A. Vagliasindi and P. Roccaro, Removal of poly- and perfluoroalkyl substances (PFAS) from water by adsorption: Role of PFAS chain length, effect of organic matter and challenges in adsorbent regeneration, *Water Res.*, 2020, **171**, 115381.

16 P. Márquez, A. Benítez, A. F. Chica, M. A. Martín and A. Caballero, Evaluating the thermal regeneration process of massively generated granular activated carbons for their reuse in wastewater treatments plants, *J. Cleaner Prod.*, 2022, **366**, 132685.

17 H. M. A. Asghar, E. P. L. Roberts, S. N. Hussain, A. K. Campen and N. W. Brown, Wastewater treatment by adsorption with electrochemical regeneration using graphite-based adsorbents, *J. Appl. Electrochem.*, 2012, **42**, 797–807.

18 J. W. Blair and G. W. Murphy, Electrochemical demineralization of water with porous electrodes of large surface area, *Adv. Chem.*, 1960, **27**(20), 206–223.

19 P. M. Biesheuvel, S. Porada, M. Levi and M. Z. Bazant, Attractive forces in microporous carbon electrodes for capacitive deionization, *J. Solid State Electrochem.*, 2014, **18**, 1365–1376.

20 Y. Liu, Y. Tian, J. Xu, C. Wang, Y. Wang, D. Yuan and J. W. Chew, Electrosorption performance on graphene-based materials: a review, *RSC Adv.*, 2023, **13**, 6518–6529.

21 N. A. Alhebshi, N. Salah, H. Hussain, Y. N. Salah and J. Yin, Structural and Electrochemical Properties of Physically and Chemically Activated Carbon Nanoparticles for Supercapacitors, *Nanomaterials*, 2021, **12**(1), 122.

22 N. Saeidi, F. Harnisch, V. Presser, F.-D. Kopinke and A. Georgi, Electrosorption of organic compounds: State of the art, challenges, performance, and perspectives, *Chem. Eng. J.*, 2023, **471**, 144354.

23 W. Deng, M. Jing, M. Gao, W. Chen, Y. Chen, F. Chen, Y. Tang and Y. Jin, The effect and mechanism of different pore structure distribution on electrosorption selectivity of anions during capacitive deionization, *Desalin. Water Treat.*, 2024, **317**, 100162.

24 X. Yang, Y. Wan, Y. Zheng, F. He, Z. Yu, J. Huang, H. Wang, Y. S. Ok, Y. Jiang and B. Gao, Surface functional groups of carbon-based adsorbents and their roles in the removal of heavy metals from aqueous solutions: A critical review, *Chem. Eng. J.*, 2019, **366**, 608–621.

25 S. Dutta, B. Gupta, S. K. Srivastava and A. K. Gupta, Recent advances on the removal of dyes from wastewater using various adsorbents: a critical review, *Mater. Adv.*, 2021, **2**, 4497–4531.

26 M. Michalska, P. Pietrzyk-Thel, K. Sobczak, M. Janssen and A. Jain, Carbon framework modification; an interesting strategy to improve the energy storage and dye adsorption, *Energy Adv.*, 2024, **3**, 1354–1366.

27 M. Kah, G. Sigmund, F. Xiao and T. Hofmann, Sorption of ionizable and ionic organic compounds to biochar, activated carbon and other carbonaceous materials, *Water Res.*, 2017, **124**, 673–692.

28 M. Brammen, P. Fraga-García and S. Berensmeier, Carbon nanotubes-A resin for electrochemically modulated liquid chromatography, *J. Sep. Sci.*, 2017, **40**, 1176–1183.

29 T. Trunzer, T. Stummvoll, M. Porzenheim, P. Fraga-García and S. Berensmeier, A carbon nanotube packed bed electrode for small molecule electrosorption: an electrochemical and chromatographic approach for process description, *Appl. Sci.*, 2020, **10**, 1133.

30 Y. Han, X. Quan, S. Chen, H. Zhao, C. Cui and Y. Zhao, Electrochemically enhanced adsorption of phenol on activated carbon fibers in basic aqueous solution, *J. Colloid Interface Sci.*, 2006, **299**, 766–771.

31 D. Röcker, T. Trunzer, J. Heilingbrunner, J. Rassloff, P. Fraga-García and S. Berensmeier, Design of 3D carbon nanotube monoliths for potential-controlled adsorption, *Appl. Sci.*, 2021, **11**, 9390.

32 O. Pastushok, F. Zhao, D. L. Ramasamy and M. Sillanpää, Nitrate removal and recovery by capacitive deionization (CDI), *Chem. Eng. J.*, 2019, **375**, 121943.

33 X. L. Zhou, T. S. Zhao, Y. K. Zeng, L. An and L. Wei, A highly permeable and enhanced surface area carbon-cloth electrode for vanadium redox flow batteries, *J. Power Sources*, 2016, **329**, 247–254.

34 A. A. Wong and M. J. Aziz, Method for comparing porous carbon electrode performance in redox flow batteries, *J. Electrochem. Soc.*, 2020, **167**, 110542.

35 B. E. Conway, E. Ayranci and H. Al-Maznai, Use of quasi-3-dimensional porous electrodes for adsorption and electrocatalytic removal of impurities from waste-waters, *Electrochim. Acta*, 2001, **47**, 705–718.

36 C. Rong and H. Xien, Reversible electrosorption of thiocyanate anions by active carbon felt, *Sep. Sci. Technol.*, 2009, **44**, 3984–3999.

37 G. Zhao, J. Li, X. Ren, C. Chen and X. Wang, Few-layered graphene oxide nanosheets as superior sorbents for heavy metal ion pollution management, *Environ. Sci. Technol.*, 2011, **45**, 10454–10462.

38 S. Chen, J. Hong, H. Yang and J. Yang, Adsorption of uranium(VI) from aqueous solution using a novel graphene oxide-activated carbon felt composite, *J. Environ. Radioact.*, 2013, **126**, 253–258.

39 Z. Li, L. Deng, I. A. Kinloch and R. J. Young, Raman spectroscopy of carbon materials and their composites: Graphene, nanotubes and fibres, *Prog. Mater. Sci.*, 2023, **135**, 101089.

40 Z. Fan, J. Ren, F. Zhang, T. Gu, S. Zhang, R.-P. Ren and Y.-K. Lv, A flexible and self-healing supercapacitor based on activated carbon cloth/MnO$_2$ composite, *J. Mater. Sci.*, 2022, **57**, 1281–1290.

41 S. Zhou, T. B. Causey, A. Hasona, K. T. Shanmugam and L. O. Ingram, Production of optically pure D-lactic acid in mineral salts medium by metabolically engineered Escherichia coli W3110, *Appl. Environ. Microbiol.*, 2003, **69**, 399–407.

42 S. E. Urbance, A. L. Pometto, A. A. Dispirito and Y. Denli, Evaluation of succinic acid continuous and repeat-batch biofilm fermentation by Actinobacillus succinogenes using plastic composite support bioreactors, *Appl. Microbiol. Biotechnol.*, 2004, **65**, 664–670.

43 M. Gheytanzadeh, A. Baghban, S. Habibzadeh, A. Mohaddespour and O. Abida, Insights into the estimation of capacitance for carbon-based supercapacitors, *RSC Adv.*, 2021, **11**, 5479–5486.

44 W. G. Pell, B. E. Conway and N. Marincic, Analysis of non-uniform charge/discharge and rate effects in porous carbon capacitors containing sub-optimal electrolyte concentrations, *J. Electroanal. Chem.*, 2000, 9–21.

45 M. Aslan, M. Zeiger, N. Jäckel, I. Grobelsek, D. Weingarth and V. Presser, Improved capacitive deionization performance of mixed hydrophobic/hydrophilic activated carbon electrodes, *J. Phys.: Condens. Matter*, 2016, **28**, 114003.

46 K. Ge, H. Shao, P.-L. Taberna and P. Simon, Understanding ion charging dynamics in nanoporous carbons for electrochemical double layer capacitor Applications, *ACS Energy Lett.*, 2023, **8**, 2738–2745.

47 P. M. Biesheuvel, Y. Fu and M. Z. Bazant, Diffuse charge and faradaic reactions in porous electrodes, *Phys. Rev. E: Stat., Nonlinear, Soft Matter Phys.*, 2011, **83**, 61507.

48 G. Ersan, Y. Kaya, O. G. Apul and T. Karanfil, Adsorption of organic contaminants by graphene nanosheets, carbon nanotubes and granular activated carbons under natural organic matter preloading conditions, *Sci. Total Environ.*, 2016, **565**, 811–817.

49 K. Delhiraja, K. Vellingiri, D. W. Boukhvalov and L. Philip, Development of Highly Water Stable Graphene Oxide-Based Composites for the Removal of Pharmaceuticals and Personal Care Products, *Ind. Eng. Chem. Res.*, 2019, **58**, 2899–2913.

50 R. Wagner, S. Bag, T. Trunzer, P. Fraga-García, W. Wenzel, S. Berensmeier and M. Franzreb, Adsorption of organic molecules on carbon surfaces: Experimental data and molecular dynamics simulation considering multiple protonation states, *J. Colloid Interface Sci.*, 2021, **589**, 424–437.

51 K. L. Tan and B. H. Hameed, Insight into the adsorption kinetics models for the removal of contaminants from aqueous solutions, *J. Taiwan Inst. Chem. Eng.*, 2017, **74**, 25–48.

52 A. H. Da Silva and E. A. Miranda, Adsorption/Desorption of Organic Acids onto Different Adsorbents for Their Recovery from Fermentation Broths, *J. Chem. Eng. Data*, 2013, **58**, 1454–1463.

53 S. Vasudevan and J. Lakshmi, The adsorption of phosphate by graphene from aqueous solution, *RSC Adv.*, 2012, **2**, 5234.

54 M. I. Hoppen, K. Q. Carvalho, R. C. Ferreira, F. H. Passig, I. C. Pereira, R. Rizzo-Domingues, M. K. Lenzi and R. Bottini, Adsorption and desorption of acetylsalicylic acid onto activated carbon of babassu coconut mesocarp, *J. Environ. Chem. Eng.*, 2019, **7**, 102862.

55 N. Schewe, R. Wagner, M. Franzreb and P. Thissen, Role of the Hydration Shell in the pH-Dependent Adsorption of Maleic Acid, *J. Phys. Chem. C*, 2021, **125**, 12305–12315.

56 R. Santoyo-Cisneros, J. R. Rangel-Mendez, J. L. Nava, E. R. Larios-Durán and L. F. Chazaro-Ruiz, Influence of surface chemistry of activated carbon electrodes on electro-assisted adsorption of arsenate, *J. Hazard. Mater.*, 2020, **392**, 122349.

57 E. Bayram, N. Hoda and E. Ayranci, Adsorption/electrosorption of catechol and resorcinol onto high area activated carbon cloth, *J. Hazard. Mater.*, 2009, **168**, 1459–1466.

58 J. Niu and B. E. Conway, Development of techniques for purification of waste waters: removal of pyridine from aqueous solution by adsorption at high-area C-cloth electrodes using *in situ* optical spectrometry, *J. Electroanal. Chem.*, 2002, **521**, 16–28.

59 K. D. Belaid, S. Kacha, M. Kameche and Z. Derriche, Adsorption kinetics of some textile dyes onto granular activated carbon, *J. Environ. Chem. Eng.*, 2013, **1**, 496–503.

60 E. Ayranci and N. Hoda, Adsorption kinetics and isotherms of pesticides onto activated carbon-cloth, *Chemosphere*, 2005, **60**, 1600–1607.

61 J.-P. Simonin, On the comparison of pseudo-first order and pseudo-second order rate laws in the modeling of adsorption kinetics, *Chem. Eng. J.*, 2016, **300**, 254–263.

62 J. J. Pignatello and B. Xing, Mechanisms of slow sorption of organic chemicals to natural particles, *Environ. Sci. Technol.*, 1996, **30**, 1–11.

63 C. Rong and H. Xien, Electrosorption of thiocyanate anions on active carbon felt electrode in dilute solution, *J. Colloid Interface Sci.*, 2005, **290**, 190–195.

64 R. Berenguer, J. P. Marco-Lozar, C. Quijada, D. Cazorla-Amorós and E. Morallón, Electrochemical regeneration and porosity recovery of phenol-saturated granular activated carbon in an alkaline medium, *Carbon*, 2010, **48**, 2734–2745.

65 E. J. Bain, J. M. Calo, R. Spitz-Steinberg, J. Kirchner and J. Axén, Electrosorption/Electrodesorption of arsenic on a granular activated carbon in the presence of other heavy metals, *Energy Fuels*, 2010, **24**, 3415–3421.

66 M. M. Sabzehmeidani, S. Mahnaee, M. Ghaedi, H. Heidari and V. A. L. Roy, Carbon based materials: a review of adsorbents for inorganic and organic compounds, *Mater. Adv.*, 2021, **2**, 598–627.

67 R. A. de Oliveira, A. Komesu, C. E. Vaz Rossell, M. R. Wolf Maciel and R. Maciel Filho, A study of the residual fermentation sugars influence on an alternative downstream process for first and second-generation lactic acid, *Sustainable Chem. Pharm.*, 2020, **15**, 100206.

68 Q. Kong, B. Xie, S. Preis, Y. Hu, H. Wu and C. Wei, Adsorption of Cd^{2+} by an ion-imprinted thiol-functionalized polymer in competition with heavy metal ions and organic acids, *RSC Adv.*, 2018, **8**, 8950–8960.

69 J. Nordstrand and J. Dutta, Predicting and enhancing the ion selectivity in multi-ion capacitive deionization, *Langmuir*, 2020, **36**, 8476–8484.

70 S. Wang, X. Li, H. Zhao, X. Quan, S. Chen and H. Yu, Enhanced adsorption of ionizable antibiotics on activated carbon fiber under electrochemical assistance in continuous-flow modes, *Water Res.*, 2018, **134**, 162–169.

71 E. Bayram and E. Ayranci, Electrosorption based waste water treatment system using activated carbon cloth electrode: Electrosorption of benzoic acid from a flow-through electrolytic cell, *Sep. Purif. Technol.*, 2012, **86**, 113–118.

72 P. Verma, *Industrial Microbiology and Biotechnology*, Springer Singapore, Singapore, 2022.